Original Article

Cardiac lesions in Duchenne muscular dystrophy model rats with out-of-frame *Dmd* gene mutation mediated by CRISPR/Cas9 system

Mao Miyamoto[1], Ryota Tochinai[1*], Shin-ich Sekizawa[1], Takanori Shiga[2], Kazuyuki Uchida[2], Yoshiharu Tsuru[3], and Masayoshi Kuwahara[1*]

[1] Department of Veterinary Pathophysiology and Animal Health, Graduate School of Agricultural and Life Sciences, The University of Tokyo, 1-1-1 Yayoi, Bunkyo-ku, Tokyo 113-8657, Japan
[2] Department of Veterinary Pathology, Graduate School of Agricultural and Life Sciences, The University of Tokyo, 1-1-1 Yayoi, Bunkyo-ku, Tokyo 113-8657, Japan
[3] Primetech Corp. Life Science Laboratory, 1-1-1 Yayoi, Bunkyo-ku, Tokyo 113-8657, Japan

Abstract: Duchenne muscular dystrophy (DMD) is a progressive muscular disorder caused by X-chromosomal *DMD* gene mutations. Recently, a new CRISPR/Cas9-mediated DMD rat model (cDMDR) was established and is expected to show cardiac lesions similar to those in humans. We therefore investigated the pathological and pathophysiological features of the cardiac lesions and their progression in cDMDR. For our cDMDR, *Dmd*-mutated rats (W-Dmd[em1Kykn]) were obtained. *Dmd* heterozygous-deficient females and wild-type (WT) males were mated, and male offspring including WT as controls were used. (1) Hearts were collected at 3, 5, and 10 months of age, and HE- and Masson's trichrome-stained specimens were observed. (2) Electrocardiogram (ECG) recordings were made and analyzed at 3, 5, and 8 months of age. (3) Echocardiography was performed at 9 months of age. In cDMDR rats, (1) degeneration/necrosis of cardiomyocytes and myocardial fibrosis prominent in the right ventricular wall and the outer layer of the left ventricular wall were observed. Fibrosis became more prominent with aging. (2) Lower P wave amplitudes and greater R wave amplitudes were detected. PR intervals tended to be shorter. QT intervals were longer at 3 months but tended to be shorter at 8 months. Sinus irregularity and premature ventricular contraction were observed at 8 months. (3) Echocardiography indicated myocardial sclerosis and a tendency of systolic dysfunction. Pathological and pathophysiological changes occurred in cDMDR rat hearts and progressed with aging, which is, to some extent, similar to what occurs in humans. Thus, cDMDR could be a valuable model for studying cardiology of human DMD. (DOI: 10.1293/tox.2020-0018; J Toxicol Pathol 2020; 33: 227–236)

Key words: dystrophin, fibrosis, cardiac necrosis, electrocardiogram, arrhythmia, echocardiogram

Introduction

Muscular dystrophy is a group of diseases characterized by degeneration and necrosis of skeletal muscles, resulting in progressive weakness and loss of muscular tissue. Its causes are mutations in the genes responsible for the structure and the functioning of the patients' muscles. It is known that there are various types of muscular dystrophy: autosomal gene mutation types such as limb-girdle muscular dystrophy and facioscapulohumeral muscular dystrophy, and X chromosome gene mutation types such as Duchenne muscular dystrophy (DMD) and Becker muscular dystrophy.

Among them, DMD is a severe type of muscular dystrophy that occurs in about 1 in 3,500 boys[1]. Dystrophin, a rod-like protein encoded by the *DMD* gene on the X chromosome, has very important roles in structural stabilization of the membrane in myocytes and providing resistance against mechanical stress by linking contact of the cytoskeleton to the basement membrane[2]. Full-length dystrophin molecules cannot be synthesized in DMD patients because of mutations in the *DMD* gene, and dystrophin deficiency causes membrane weakness in skeletal myocytes and myocardial cells that leads to cardiorespiratory issues and eventually death. One of the most common causes of muscular dystrophy-related deaths is currently heart failure brought on by myocardial damage instead of respiratory failure[3].

So far, animal models have been established using mice and dogs to elucidate the pathogenesis of DMD and to develop therapeutic methods. It has become apparent, however, that these animal models have certain disadvantages in terms of human DMD studies[4–6]. The canine X-linked muscular dystrophy (CXMD) model shows similar pathological findings as in human DMD patients, but phenotypes can vary between individuals and laborious efforts are required

for breeding and to maintain this model[6]. Meanwhile, X-linked muscular dystrophy (*mdx*) mice can be easily bred and maintained as a model, but their pathological changes are milder than those in human DMD patients[7–9].

Yamanouchi and his colleagues recently established a DMD rat model using the CRISPR/Cas9 system[10]. It is reported that this rat model lacks dystrophin. Fibrosis of the diaphragm and the tibialis muscle becomes significantly more prominent from the age of 3 months and progresses thereafter. In addition, progressive weight loss and kyphosis are seen from approximately 6 months of age. Although the lifespan of these rats has not been fully evaluated yet, by the time they reach 10 months of age, body weight loss becomes apparent, and they are no longer suitable for breeding. It has been confirmed by histopathological analysis using Masson's trichrome stain that these rats show ventricular fibrosis with infiltration of inflammatory cells at 3 months of age; however, no reports on the progression of such heart lesions have been made yet.

In human DMD patients, various cardiac changes have been reported and characterized, including supraventricular tachycardia, ventricular tachycardia, premature ventricular contraction, atrioventricular block, heart rate increase, QT interval prolongation, QRS duration prolongation, PR interval shortening, increase in R wave amplitude, myocardial fibrosis, and dilated cardiomyopathy[11–15]. It is also reported that parasympathetic nervous function is reduced in human DMD patients[16]. However, whether these pathophysiological changes and disease/lesion progression seen in human DMD patients also take place in this DMD rat model remains largely unknown.

In this study, the progression of cardiac lesions over time in the novel DMD rat model was evaluated through histopathological and electrocardiological methods. In addition, cardiac function was analyzed using echocardiography, in order to understand pathological and pathophysiological features of this DMD rat model.

Materials and Methods

Ethics

All experiments using rats were conducted in accordance with the Animal Experimentation Guidelines of the University of Tokyo and were approved by the Institutional Animal Care and Use Committee of the Graduate School of Agricultural and Life Sciences at the University of Tokyo.

Animals

Rats with gene mutations induced by the clustered regularly interspaced short palindromic repeats (CRISPR) system, an RNA-based genomic targeting tool, were used. Colonies of CRISPR/Cas9-mediated *Dmd*-mutated rats[10] (W-Dmd*[emlKykn]*; cDMDR) and their wild type (WT) were established and maintained by the Department of Veterinary Physiology, Graduate School of Agricultural and Life Sciences, The University of Tokyo, and our lab obtained several rats for breeding. cDMDR have out-of-frame muta-

tions in *Dmd* gene exons (329 bases deficiency in exon 3 to intron 3, exon 16: 5'-GCACAt*A(AT)#GG-3', *: 1 base insertion, #: 2 bases substitution), which result in the absence of dystrophin expression. It is known that the average life expectancy of many DMD patients is around 26 years, with the aid of a ventilator because of respiratory and heart failure, but some can live into middle age and possibly longer with a help of gene therapies[17]. Therefore, in this study, we focused on the rats from 3 to 8/10 months of age, which can be relevant to human age from young adult to middle age, respectively[18]. Male offspring bred in our laboratory were used in this study. They were housed in plastic cages in a controlled environment (light-dark cycle 12/12 h, temperature 23 ± 3°C) with ad libitum access to laboratory basal feed and tap water.

Evaluation of histopathological changes

3-, 5-, or 10-month-old cDMDR (n = 3/each age group), and 10-month-old WT (n = 2) rats were anesthetized with isoflurane and necropsy was performed. After exsanguination, their hearts were removed and immediately fixed in 10% neutral phosphate-buffered formalin. The fixed hearts were cross-sectioned at three planes through the ventricles and embedded in paraffin before being sectioned to obtain 4 μm-thick specimens. The specimens were stained with hematoxylin and eosin (HE) or Masson's trichrome. For immunohistochemical staining, an anti-dystrophin mouse monoclonal antibody (clone: 6D3, Merck Millipore, MA, USA) was used, followed by a horseradish peroxidase-labeled secondary antibody, and staining results were visualized with 3.3'-diaminobenzidine. Observation of these specimens was performed using a light microscope. In addition, the fibrosis area was calculated for all the three Masson's trichrome-stained ventricular slides using an image processing program (ImageJ, National Institute of Health, MD, USA).

Evaluation of electrocardiogram (ECG)

ECG waveforms were analyzed in accordance with our previous report with some modifications[19]. At 3, 5 or 8 months of age (sample size provided in Fig. 5), rats were anesthetized with isoflurane and placed in a prone position after measuring body weight. Needle electrodes were then placed on each limb in order to record limb lead ECG. The electrodes were connected to an ECG processor (EP95U, Softron, Tokyo, Japan) via transducer amplification equipment (Nippon Denki San-ei, Tokyo, Japan), and electric potential was sampled every 1 ms. All ECG data analysis was performed using ECG analyzing software (SRV2W and SP-2000U, Softron, Tokyo, Japan).

Evaluation of cardiac function

At 9 months of age (n = 5 for the cDMDR group and n = 2 for the WT group), body weight was measured. Under isoflurane anesthesia, echocardiography was recorded using a preclinical imaging system (Vevo®3100, FUJIFILM VisualSonics, Toronto, Canada) in accordance with our previous

report with some modifications[20]. Left-ventricular short-axis-waveforms and left-ventricular inflow-waveforms were analyzed, and heart rate, left ventricular mass, stroke volume, ventricular wall thickness (left anterior wall [LVAW], and left posterior wall [LVPW]), mitral valve early diastolic filling velocity [E wave]/atrial filling velocity [A wave] (MV E/A), ejection fraction, fractional shortening, and cardiac output were calculated using analysis software (Vevo LAB, FUJIFILM VisualSonics, Toronto, ON, Canada).

Statistics

Differences in fibrosis area among the three age groups of cDMDR rats were analyzed using one-way ANOVA followed by Tukey's test. Differences in ECG components between WT and cDMDR were analyzed using two-way ANOVA followed by Student's *t*-tests. Results were considered statistically significant when p<0.05. All statistical analyses were performed with Excel 2019 (Microsoft Corp., Redmond, WA, USA) and EZR[21] (Saitama Medical Center, Jichi Medical University, Saitama, Japan), which is a graphical user interface for R (The R Foundation for Statistical Computing, Vienna, Austria).

Results

Evaluation of histopathological changes in cDMDR

At 3, 5, and 10 months of age, cDMDR hearts were negative for dystrophin (Fig. 1) and showed degeneration/necrosis of myocardial cells, infiltration of mononuclear cells, and fibrosis (Fig. 2). These myocardial lesions were prominent in the right ventricular wall and the outer layer of the left ventricular wall. While the combination of observed findings was similar between age groups, fibrosis significantly advanced with aging (Fig. 3). Histopathological findings indicative of hypertrophic cardiomyopathy or dilated cardiomyopathy, which are seen in human DMD, were not apparent.

Evaluation of ECG

The typical ECG waveforms of arrhythmias observed in cDMDR are shown in Fig. 4. Sinus irregularities and premature ventricular contraction were observed in cDMDR, whereas these arrhythmias were not detected in WT animals (Table 1).

Although statistical detection sensitivity differed between age groups because the number of samples per age group varied, ECG waveform analysis did show some significant differences among them (Fig. 5). P wave amplitudes tended to be smaller at 8 months of age in the cDMDR group. R wave amplitudes were significantly larger, while PR intervals tended to be shorter at 3 and 8 months of age in the cDMDR group. At 3 months of age, QT intervals in cDMDR rats were significantly longer but tended to be shorter at 8 months of age.

Evaluation of cardiac function

In B-mode images of left ventricles of cDMDR rats, some high brightness lesions suggesting sclerosis were observed in the sub-epicardium and the papillary muscle (Fig. 6). Left ventricular mass and left ventricular wall thickness did not clearly differ between cDMDR and WT groups (Fig. 7B, D, and E). However, systolic parameters such as stroke volume, ejection fraction, fractional shortening, and cardiac output tended to be reduced in cDMDR animals (Fig. 7C, G, H, and I). Moreover, MV E/A tended to be higher in cDMDR rats (Fig. 7F). The change in MV E/A could be a result of systolic failure because the early diastolic filling velocity (E-wave) increases when the left ventricle sclerosis and contractility decreases.

Discussion

Dystrophin contributes to the stabilization of the plasma membrane structure by connecting the myocyte cytoskeleton to the basement membrane. It is considered that the cell membrane of the cardiomyocyte becomes weak because of dysfunctional dystrophin, consequently leading to the degeneration and necrosis of the cardiomyocyte. The pathological myocardial changes in cDMDR were broadly distributed but particularly prominent in the right ventricular wall and the outer layer of the left ventricular wall. It is widely known that progressive cardio-myopathy (PCM) occurs in many strains of rats and mice, and its typical distribution, namely the predilection for the left ventricle, subendocardial regions, and the apex of the heart, has supported a hypothesis on pathogenesis related to ischemia and vascular diseases[22]. However, the lesions in cDMDR were distributed in the right ventricular wall and the outer layer of the left ventricular wall. This pattern of lesion distribution implies that the lesions were different from PCM and were not induced of ischemic (vascular) origins but were of myocardial cellular origin[22].

In an earlier study, a TALEN-mediated DMD rat (tDMDR) model was created[23]. Although Larcher *et al.* reported that degeneration/necrosis of myocardial cells, infiltration of mononuclear cells, and fibrosis were detected in tDMDR, the lesion distribution in tDMDR hearts has not been reported in detail to date. In the current study, it was revealed

Table 1. Arrhythmia Incidences in Anesthetized Rats at Different Ages

| age	3 months		5 months		8 months	
type	WT	cDMDR	WT	cDMDR	WT	cDMDR
sinus irregularity	0/8	0/9	0/5	0/4	0/4	2/3
premature ventricular contraction	0/8	0/9	0/5	1/4	0/4	1/3
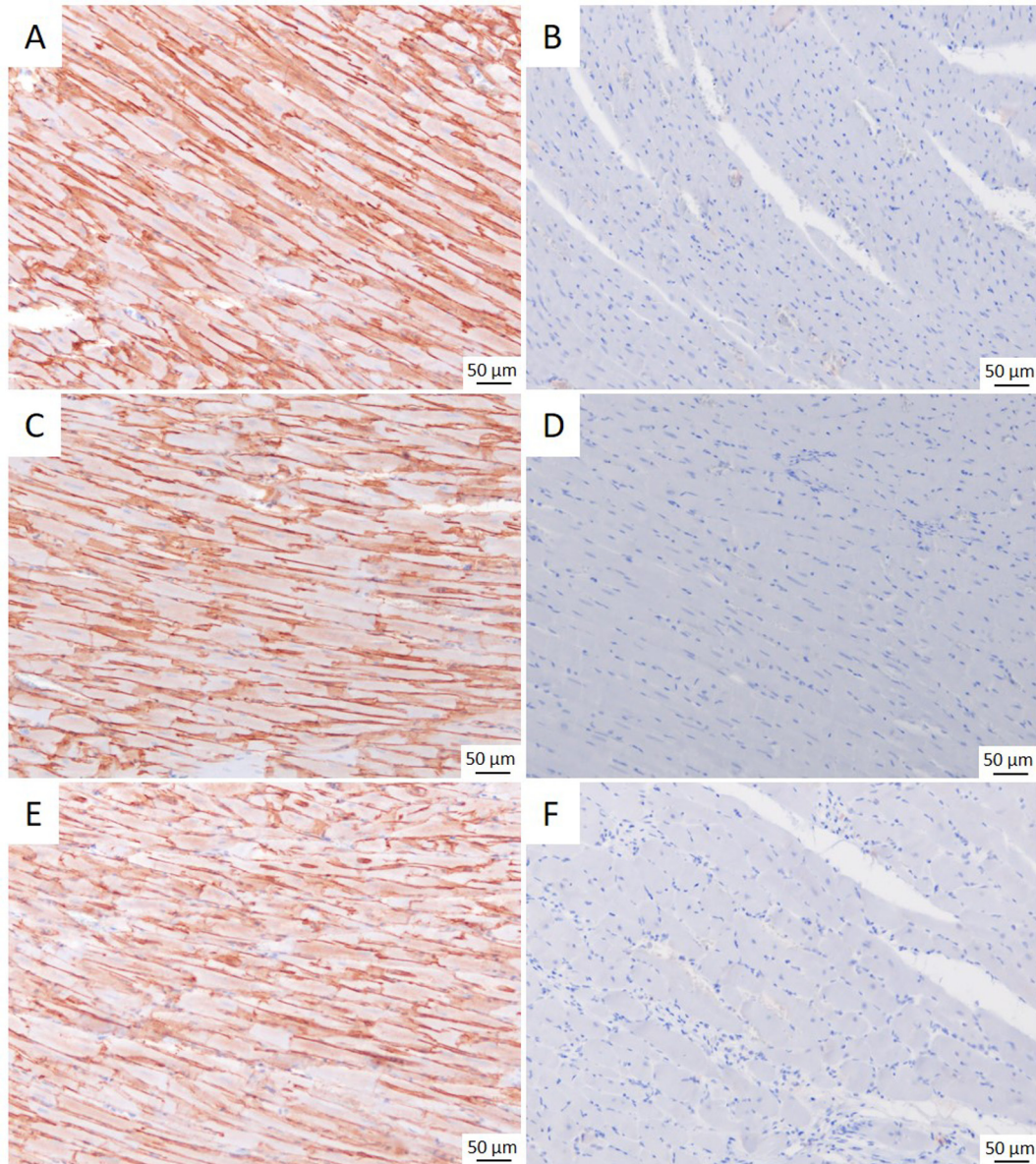
Fig. 1. Immunohistochemical staining of hearts (left ventricles) with anti-dystrophin mouse monoclonal antibody. Dystrophin staining is clearly found especially in the membrane of cardiomyocytes of wild type rats (A, C and E) while there is no staining in the hearts at any age of cDMDR rats (B, D, and F). A: WT at 3 months of age. B: cDMDR at 3 months of age. C: WT at 5 months of age. D: cDMDR at 5 months of age. E: WT at 10 months of age. F: cDMDR at 10 months of age.

that the lesion distribution pattern for cDMDR hearts was mostly the same as that observed in human DMD[24]. In addition, pathological findings in cDMDR were almost in conformity with those in human DMD[12–14, 24, 25]. Furthermore, a tendency of systolic dysfunction in the hearts of cDMDR rats could be detected in this study, which was not reported in tDMDR[23].

Pathological myocardial lesions do not seem to be obvious in DMD model mice[7]. For example, Torres and Duchen did not detect pathological changes in heart muscle samples from *mdx* mice[26], and Megeney *et al.* reported that *mdx* mice rarely display histological changes in cardiac tissues[27]. Although *mdx* mice at 10–12 months of age exhibited necrosis

and fibrosis of the cardiac muscle[9], these lesions seem to be milder than those seen in cDMDR in the present study. From these aspects, cDMDR has a number of characteristics in common with human DMD, which were not present in the mouse or other rat models, and the model may be considered as a valuable animal model that could mimic DMD disease states closer to humans.

Compared to human DMD patients and DMD dog models, myocardial lesions were considered to be milder in cDMDR because severe cardiomyopathy such as hypertrophic or dilated cardiomyopathy, which are seen in human DMD patients and DMD dog models, were not apparent from pathological and echocardiographic studies. Whereas
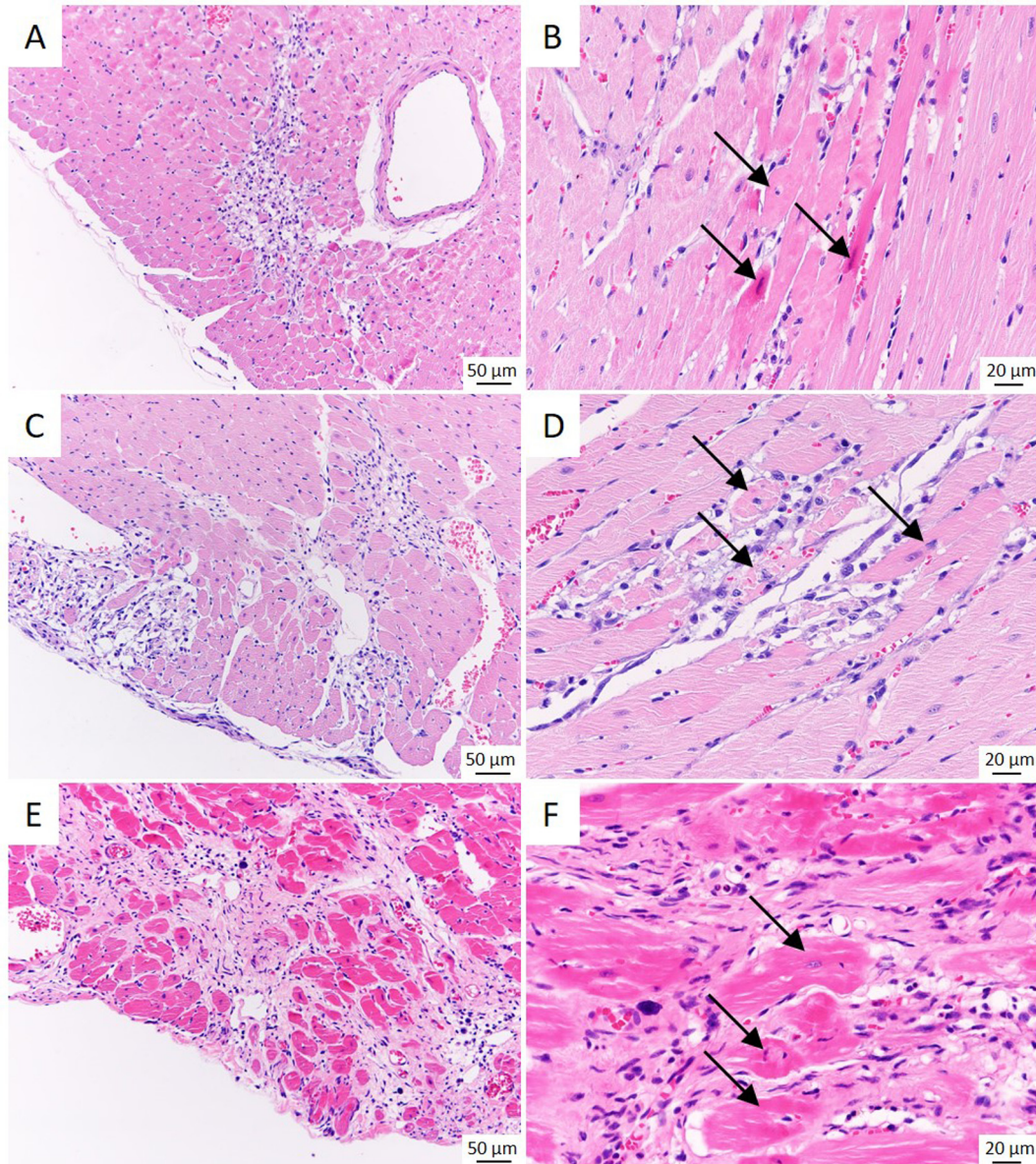
Fig. 2. Histopathological changes in cDMDR hearts. Cardiomyocyte degeneration and necrosis, mononuclear cell infiltration, and fibrosis are observed in all age groups. These changes are found diffusely in the ventricular wall and papillary muscle, and especially prominent in the right ventricular wall and the outer layer of the left ventricular wall. There are, to some degree, differences in the lesions between cDMDR of the same age, but histopathological findings are similar for all cDMDR. There are no apparent histopathological findings indicative of hypertrophic cardiomyopathy or dilated cardiomyopathy. A, B: Left ventricle of cDMDR at 3 months of age. Arrows indicate necrosis of cardiomyocytes. C, D: Left ventricle of cDMDR at 5 months of age. Arrows indicate necrosis of cardiomyocytes. E, F: Left ventricle of cDMDR at 10 months of age. Arrows indicate necrosis of cardiomyocytes. A–F: HE stain.

the degree of the heart and muscular lesions of DMD dog models can vary between individuals, cDMDR lesions showed less pathological variations between individuals (Fig. 3), which would be a great advantage for DMD research. Overall, it seems that cDMDR might serve a good model for DMD research, especially for initial and/or low-grade disease stages with similar lesions to human DMD patients, even though the cDMDR may have some limitations for studying the precise mechanisms of human DMD.

The following factors are presumed to be involved in the ECG changes in cDMDR rats. Figure 3 shows an increase in fibrosis area in cDMDR hearts with aging, while several ECG parameters did not change age-dependently. ECG parameters other than P wave amplitude may therefore not be an index of DMD disease progression. Changes in these two parameters may indicate severity of myocardial lesions in the atrium and the ventricle, respectively. Unfortunately, changes in these two ECG parameters were not consistent with changes observed in human DMD patients, but it is possible that some of the ECG parameters could
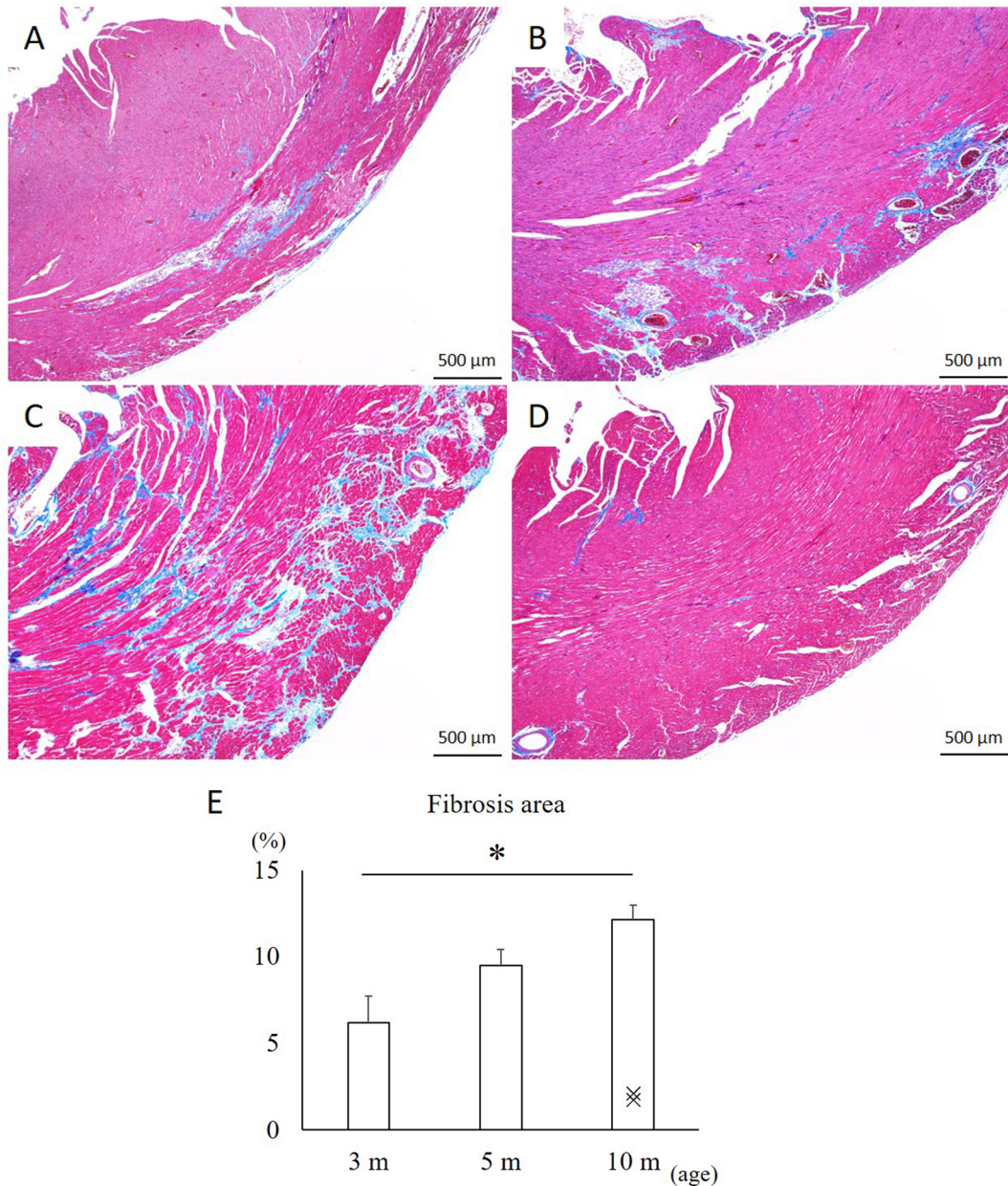
Fig. 3. Progression of fibrosis with aging in cDMDR rats. Masson's-trichrome stain of the heart indicates progression of fibrosis from 3 to 5 and 10 months of age in cDMDR rats (A-C, respectively) but minimal changes in 10-month-old WT rats (D). The percentage of fibrosis area in the overall cross-sectional area of the heart increased with aging (E). Bars indicate Mean $\pm$ SE of cDMDR (n = 3/group). X-marks indicate individual values of WT rats at 10 months of age (n = 2). *: $p < 0.05$ (the difference among three age groups of cDMDR). Post-hoc Tukey's test following one-way ANOVA.
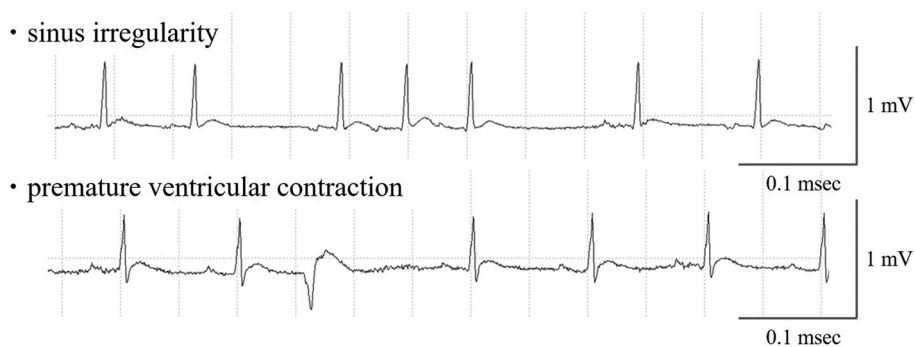
Fig. 4. Electrocardiographic waveforms of arrhythmias observed in cDMDR
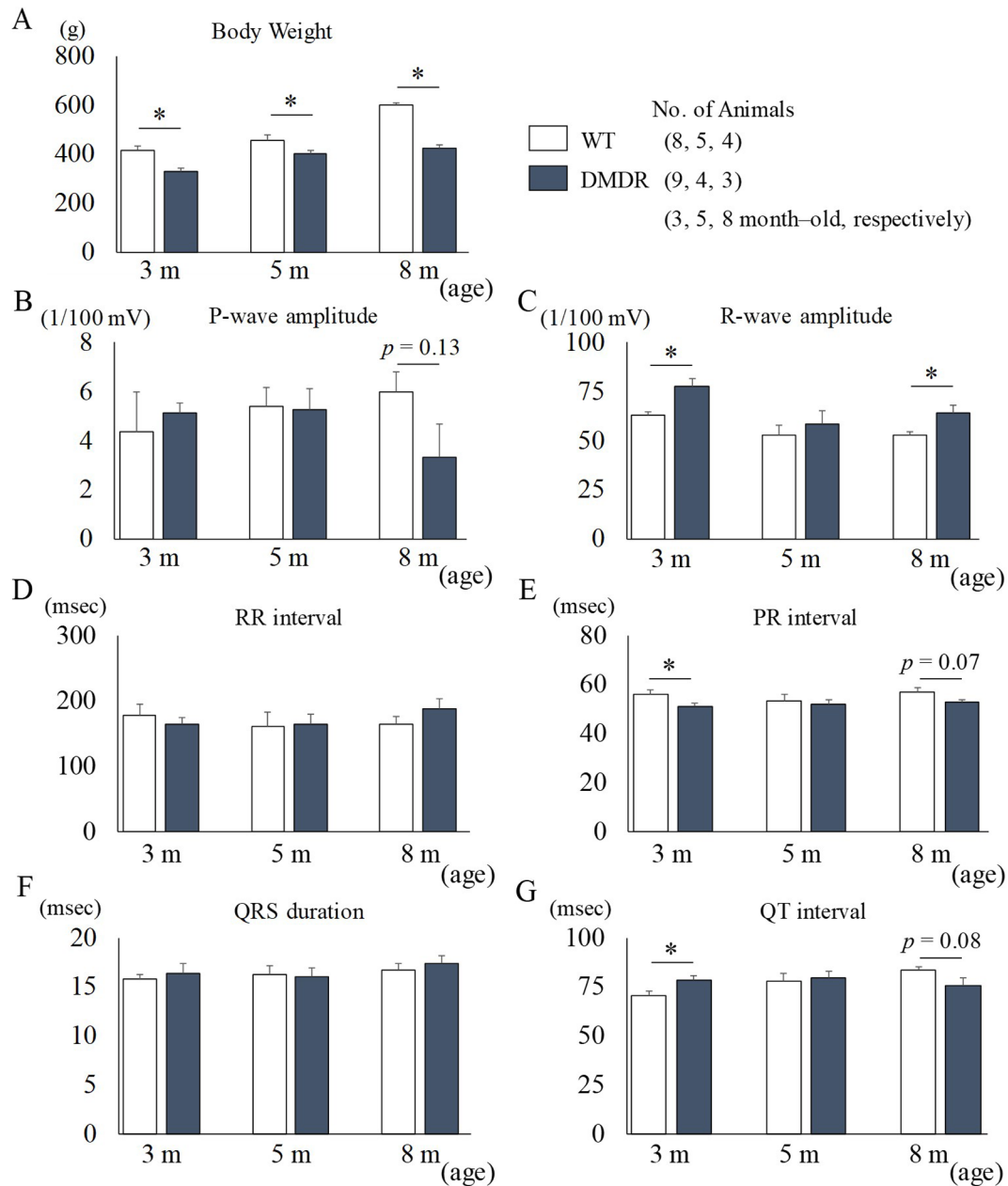
Fig. 5. Body weight and electrocardiographic waveform components in cDMDR and WT rats at different ages. Greater R-wave amplitudes and shorter PR-intervals in cDMDR rats can be seen, albeit with differences in statistical detection sensitivity between age group caused by the difference in the number of samples per age group. A prolonged QT interval at 3 months of age but a trend toward shorter QT interval at 8 months of age are observed, and a trend toward lower P wave amplitudes at 8 months of age is detected in cDMDR. Mean ± SE, *: $p < 0.05$. Post-hoc Student's *t*-test following two-way ANOVA.

serve as biomarkers for new therapeutic strategies such as oligonucleotide-mediated exon skipping therapy using eteplirsen and golodirsen, both approved by United States Food and Drug Administration[28, 29].

Degeneration/necrosis of cardiomyocytes and fibrosis contribute to the deterioration of sinus functions, the cardiac conduction system, and the conduction between ventricular cardiomyocytes. Reduced sinus function leads to bradycardia, decreased P wave amplitude, and abnormal sinus rhythm (sinus irregularity). Conduction system disorder

leads to PR interval prolongation, and conduction abnormality between cardiomyocytes in the ventricle leads to QRS duration prolongation, QT interval prolongation, and premature ventricular contraction. Tissue changes of the heart seemed to reduce cardiac function. In fact, changes in the parameters of cardiac function in cDMDR suggested systolic dysfunction. Therefore, it can be considered that compensatory changes to reduce cardiac function might cause increases in sympathetic nervous activity. In human DMD patients, it is also known that sympathetic nervous activity
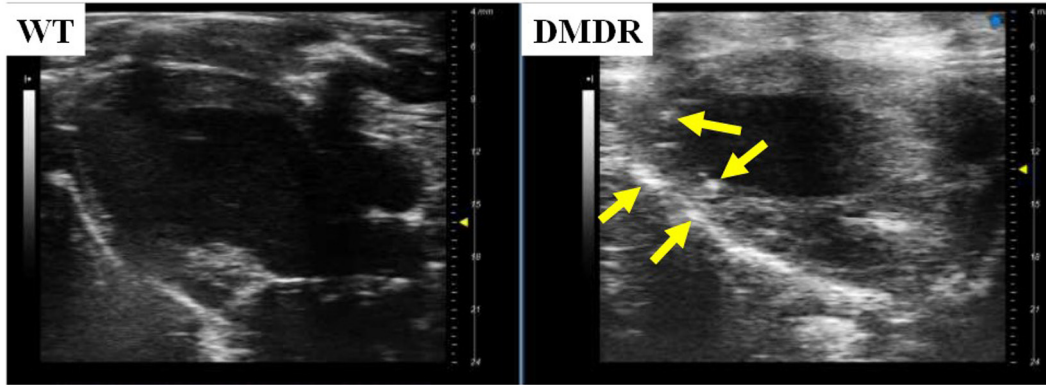
Fig. 6. Left ventricular long-axis cross-sectional imaging (B-Mode) from cDMDR and WT at 9 months of age. Very bright echoed areas (arrows) in the subadventitia and near the papillary muscles indicate tissue sclerosis in cDMDR.
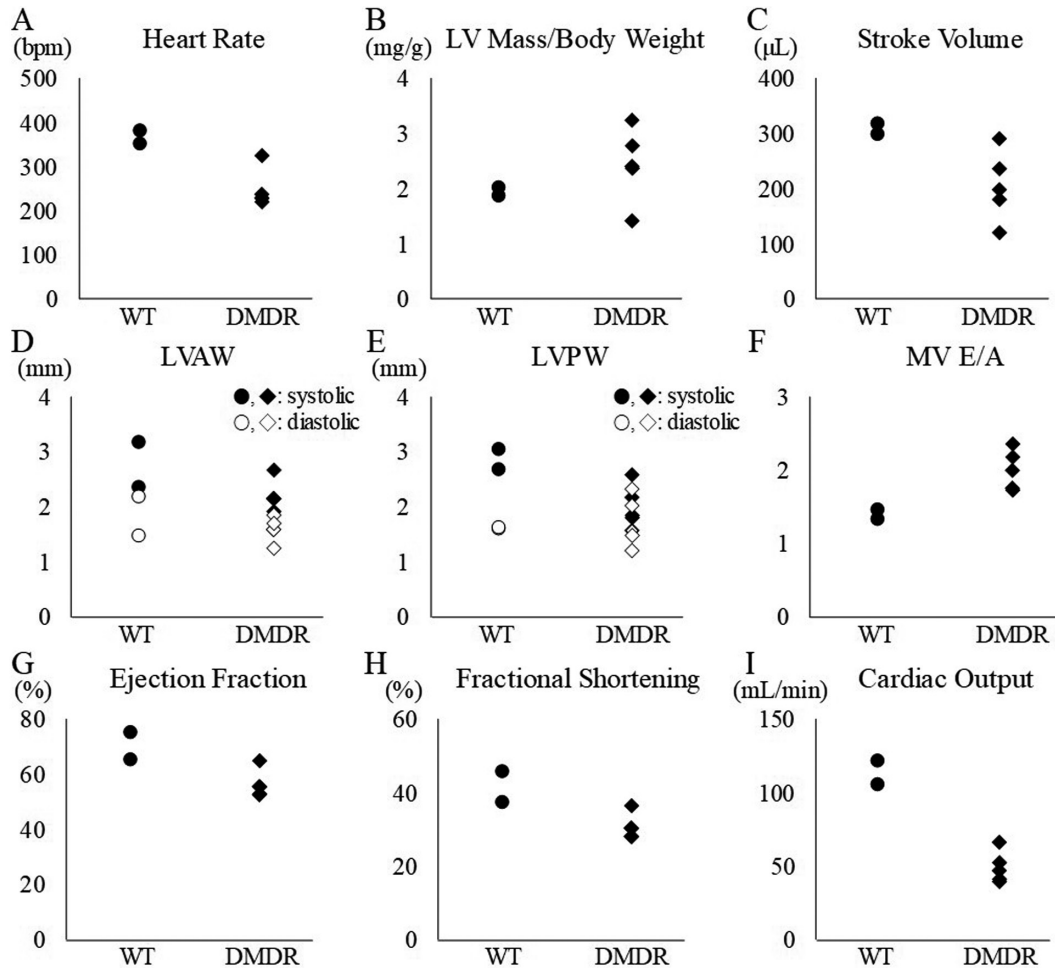
Fig. 7. Individual data from echo images in cDMDR and WT rats. A: Heart rate; B: Left ventricular wall weight/body weight ratio; C: Stroke volume; D: Left ventricular anterior wall thickness; E: Left ventricular posterior wall thickness; F: Ratio of left ventricular rapid inflow velocity (E-wave) to atrial systolic inflow velocity (A-wave); G: Left ventricular ejection fraction; H: Left ventricular internal diameter fractional shortening; I: Cardiac output. Note that tendency toward worsening of contractile indices (C, G, H, and I) as well as a tendency toward worsening of diastolic function (F) are seen.

becomes predominant compared to parasympathetic activity. The increase in sympathetic nervous activity seems to induce the increase in heart rate and the decrease in PR interval, QRS duration, and QT interval. Furthermore, weight loss was observed in cDMDR, and as weight loss reduces the electrical resistance of body tissues, surface ECG might have shown increased amplitudes for P waves and Q waves. Thus, it can be considered that ECG changes in cDMDR are induced by the combination of organic changes and the physiological events that follow. These changes also mimic the disease state of human DMD.

In this study, no histopathological analysis was performed in the atrium. In 3-month-old cDMDR, changes in P wave morphology were not apparent. However, at 8 months of age, a decrease in P wave amplitude and sinus irregularity were detected, and these ECG findings suggest functional changes in the atrium: the decrease in the amplitude of the action potential in atrial myocardial cells. Further studies with histopathological analyses of the atrium will provide us important information to understand the pathology and pathophysiology of DMD.

Tissue sclerosis was clearly detected by echocardiography in the sub-epicardium and the papillary muscle in cDMDR at 9 months of age. This was consistent with our histopathological observations such as degeneration/necrosis of cardiomyocytes and fibrosis of myocardium. As expected, stroke volume as well as cardiac output were considerably suppressed in cDMDR. Although cardiac output was significantly blunted in cDMDR, this does not necessarily mean that these animals were hypoxic. The basal respiratory function in cDMDR did not seem to be different from that in WT, and therefore the whole body may be able to receive enough oxygen to survive longer than 9 months of age, free of critical incidents observed in human DMD patients[30].

In conclusion, pathological and pathophysiological changes in the heart common with those seen in human DMD patients were detected in cDMDR. The disease severity progressed in an age-related manner, albeit milder than that in human DMD, and cDMDR rats seem to have the potential to become a useful model for human DMD research.

References

1. About Duchenne Muscular Dystrophy, from National Institutes of Health. National Human Genome Research Institute website, accessed May 28, 2020: https://www.genome.gov/Genetic-Disorders/Duchenne-Muscular-Dystrophy.
2. Petrof BJ, Shrager JB, Stedman HH, Kelly AM, and Sweeney HL. Dystrophin protects the sarcolemma from stresses developed during muscle contraction. Proc Natl Acad Sci USA. **90**: 3710–3714. 1993. [Medline] [CrossRef]
3. Kieny P, Chollet S, Delalande P, Le Fort M, Magot A, Pereon Y, and Perrouin Verbe B. Evolution of life expectancy of patients with Duchenne muscular dystrophy at AFM Yolaine de Kepper centre between 1981 and 2011. Ann Phys Rehabil Med. **56**: 443–454. 2013. [Medline] [CrossRef]
4. Banks GB, and Chamberlain JS. The value of mammalian models for duchenne muscular dystrophy in developing therapeutic strategies. Curr Top Dev Biol. **84**: 431–453. 2008. [Medline] [CrossRef]
5. Nakamura A, and Takeda S. Mammalian models of Duchenne Muscular Dystrophy: pathological characteristics and therapeutic applications. J Biomed Biotechnol. **2011**: 184393. 2011. [Medline] [CrossRef]
6. Wells DJ. Tracking progress: an update on animal models for Duchenne muscular dystrophy. Dis Model Mech. **11**: dmm035774. 2018. [Medline] [CrossRef]
7. Chu V, Otero JM, Lopez O, Sullivan MF, Morgan JP, Amende I, and Hampton TG. Electrocardiographic findings in mdx mice: a cardiac phenotype of Duchenne muscular dystrophy. Muscle Nerve. **26**: 513–519. 2002. [Medline] [CrossRef]
8. Branco DM, Wolf CM, Sherwood M, Hammer PE, Kang PB, and Berul CI. Cardiac electrophysiological characteristics of the mdx (5cv) mouse model of Duchenne muscular dystrophy. J Interv Card Electrophysiol. **20**: 1–7. 2007. [Medline] [CrossRef]
9. Masubuchi N, Shidoh Y, Kondo S, Takatoh J, and Hanaoka K. Subcellular localization of dystrophin isoforms in cardiomyocytes and phenotypic analysis of dystrophin-deficient mice reveal cardiac myopathy is predominantly caused by a deficiency in full-length dystrophin. Exp Anim. **62**: 211–217. 2013. [Medline] [CrossRef]
10. Nakamura K, Fujii W, Tsuboi M, Tanihata J, Teramoto N, Takeuchi S, Naito K, Yamanouchi K, and Nishihara M. Generation of muscular dystrophy model rats with a CRISPR/Cas system. Sci Rep. **4**: 5635. 2014. [Medline] [CrossRef]
11. Chiang DY, Allen HD, Kim JJ, Valdes SO, Wang Y, Pignatelli RH, Lotze TE, and Miyake CY. Relation of cardiac dysfunction to rhythm abnormalities in patients with Duchenne or Becker muscular dystrophies. Am J Cardiol. **117**: 1349–1354. 2016. [Medline] [CrossRef]
12. Villa CR, Czosek RJ, Ahmed H, Khoury PR, Anderson JB, Knilans TK, Jefferies JL, Wong B, and Spar DS. Ambulatory monitoring and arrhythmic outcomes in pediatric and adolescent patients with Duchenne muscular dystrophy. J Am Heart Assoc. **5**: e002620. 2015. [Medline]
13. Segawa K, Komaki H, Mori-Yoshimura M, Oya Y, Kimura K, Tachimori H, Kato N, Sasaki M, and Takahashi Y. Cardiac conduction disturbances and aging in patients with Duchenne muscular dystrophy. Medicine (Baltimore). **96**: e8335. 2017. [Medline] [CrossRef]
14. Thomas TO, Morgan TM, Burnette WB, and Markham LW. Correlation of heart rate and cardiac dysfunction in Duchenne muscular dystrophy. Pediatr Cardiol. **33**: 1175–1179. 2012. [Medline] [CrossRef]
15. Nigro G, Comi LI, Politano L, and Bain RJI. The incidence and evolution of cardiomyopathy in Duchenne muscular dystrophy. Int J Cardiol. **26**: 271–277. 1990. [Medline]

[CrossRef]

16. Lanza GA, Dello Russo A, Giglio V, De Luca L, Messano L, Santini C, Ricci E, Damiani A, Fumagalli G, De Martino G, Mangiola F, and Bellocci F. Impairment of cardiac autonomic function in patients with Duchenne muscular dystrophy: relationship to myocardial and respiratory function. Am Heart J. **141**: 808–812. 2001. [Medline] [CrossRef]

17. Lisak RP, Truong Daniel DT, and Carroll W. International Neurology: A Clinical Approach. Wiley, New Jersey. 2009.

18. Sengupta P. The Laboratory Rat: Relating Its Age With Human's. Int J Prev Med. **4**: 624–630. 2013. [Medline]

19. Tochinai R, Nagata Y, Ando M, Hata C, Suzuki T, Asakawa N, Yoshizawa K, Uchida K, Kado S, Kobayashi T, Kaneko K, and Kuwahara M. Combretastatin A4 disodium phosphate-induced myocardial injury. J Toxicol Pathol. **29**: 163–171. 2016. [Medline] [CrossRef]

20. Tochinai R, Komatsu K, Murakami J, Nagata Y, Ando M, Hata C, Suzuki T, Kado S, Kobayashi T, and Kuwahara M. Histopathological and functional changes in a single-dose model of combretastatin A4 disodium phosphate-induced myocardial damage in rats. J Toxicol Pathol. **31**: 307–313. 2018. [Medline] [CrossRef]

21. Kanda Y. Investigation of the freely available easy-to-use software 'EZR' for medical statistics. Bone Marrow Transplant. **48**: 452–458. 2013. [Medline] [CrossRef]

22. Berridge BR, Mowat V, Nagai H, Nyska A, Okazaki Y, Clements PJ, Rinke M, Snyder PW, Boyle MC, and Wells MY. Non-proliferative and proliferative lesions of the cardiovascular system of the rat and mouse. J Toxicol Pathol. **29**(Suppl): 1S–47S. 2016. [Medline] [CrossRef]

23. Larcher T, Lafoux A, Tesson L, Remy S, Thepenier V, François V, Le Guiner C, Goubin H, Dutilleul M, Guigand L, Toumaniantz G, De Cian A, Boix C, Renaud JB, Cherel Y, Giovannangeli C, Concordet JP, Anegon I, and Huchet C. Characterization of dystrophin deficient rats: a new model for Duchenne muscular dystrophy. PLoS One. **9**: e110371. 2014. [Medline] [CrossRef]

24. Frankel KA, and Rosser RJ. The pathology of the heart in progressive muscular dystrophy: epimyocardial fibrosis. Hum Pathol. **7**: 375–386. 1976. [Medline] [CrossRef]

25. Nomura H, and Hizawa K. Histopathological study of the conduction system of the heart in Duchenne progressive muscular dystrophy. Acta Pathol Jpn. **32**: 1027–1033. 1982. [Medline]

26. Torres LFB, and Duchen LW. The mutant mdx: inherited myopathy in the mouse. Morphological studies of nerves, muscles and end-plates. Brain. **110**: 269–299. 1987. [Medline] [CrossRef]

27. Megeney LA, Kablar B, Perry RLS, Ying C, May L, and Rudnicki MA. Severe cardiomyopathy in mice lacking dystrophin and MyoD. Proc Natl Acad Sci USA. **96**: 220–225. 1999. [Medline] [CrossRef]

28. FDA-Approved Drugs, from U.S. Food and Drug Administration website, accessed May 28, 2020: https://www.accessdata.fda.gov/scripts/cder/daf/index.cfm?event=overview.process&varApplNo=206488.

29. FDA-Approved Drugs, from U.S. Food and Drug Administration website, accessed May 28, 2020: https://www.accessdata.fda.gov/scripts/cder/daf/index.cfm?event=overview.process&varApplNo=211970.

30. Finder JD, Birnkrant D, Carl J, Farber HJ, Gozal D, Iannaccone ST, Kovesi T, Kravitz RM, Panitch H, Schramm C, Schroth M, Sharma G, Sievers L, Silvestri JM, Sterni L, American Thoracic Society. Respiratory care of the patient with Duchenne muscular dystrophy: ATS consensus statement. Am J Respir Crit Care Med. **170**: 456–465. 2004. [Medline] [CrossRef]